Inorg. Chem. **2007**, *46*, 2836–2845

Synthesis, Structure, and Reactivity of Mononuclear Re(I) Oximato Complexes

Luciano Cuesta,[†] Miguel A. Huertos,[†] Dolores Morales,[†] Julio Pérez,*[,†] Lucía Riera,[†] Víctor Riera,[†] Daniel Miguel,[‡] Amador Menéndez-Velázquez,[§,£] and Santiago García-Granda[||]

Departamento de Química Orgánica e Inorgánica -IUQOEM, Facultad de Química, Universidad de Oviedo-CSIC, 33006 Oviedo, Spain, Departamento de Química Inorgánica, Facultad de Ciencias, Universidad de Valladolid, 47005 Valladolid, Spain, Instituto de Ciencia de Materiales de Madrid, CSIC, Cantoblanco Ctra de Colmenar Km 15, 28049 Madrid, Spain, SpLine, European Synchrotron Radiation Facility, 6 rue Jules Horowit, BP 220, F-38043 Grenoble CEDEX, France, and Departamento de Química Física y Analítica, Facultad de Química, Universidad de Oviedo, 33006 Oviedo, Spain

Received November 14, 2006

Complexes [Re(ONCMe$_2$)(CO)$_3$(bipy)] (**1**) and [Re(ONCMe$_2$)(CO)$_3$(phen)] (**2**), synthesized by reaction of the respective triflato precursors [Re(OTf)(CO)$_3$(N–N)] (N–N = bipy, phen) with KONCMe$_2$, feature O-bonded monodentate oximato ligands. Compound [Re(CO)$_3$(phen)(HONCMe$_2$)]BAr′$_4$ (**3**), with a monodentate N-bonded oxime ligand, was prepared by reaction of [Re(OTf)(CO)$_3$(phen)], HONCMe$_2$, and NaBAr′$_4$. Deprotonation of **3** afforded **2**. The oximato complexes reacted with *p*-tolylisocyanate, *p*-tolylisothiocyanate, maleic anhydride, and tetracyanoethylene, affording the products of the insertion of the electrophile into the Re–O bond, compounds **4**–**7**. One representative of each type of compound was fully characterized, including single-crystal X-ray diffraction. The reactions of **1** and **2** with dimethylacetylenedicarboxylate were found to involve first an insertion as the ones mentioned above but followed by incorporation of water, loss of acetone, and formation of the charge-separated neutral amido complexes **9** and **10**. The structure of **9** and **10** was determined by X-ray diffraction, and key features of their electronic distribution were studied using a topological analysis of the electron density as obtained from the Fourier map.

Introduction

Due to the presence of lone electron pairs on the adjacent oxygen and nitrogen atoms, oximato ligands have been found to be able to adopt several different coordination modes.[1] The tendency of the ligand to act as a bridge between two or more metals results in that many oximato complexes are polynuclear species. In particular, this is the most common situation for transition metal carbonyl complexes, the ones more pertinent to this work.[2] Most mononuclear carbonyl complexes containing oximato ligands are of the type [MCp{ONC(R)R′}(CO)$_3$] (M = Mo, W; Cp = η^5-cyclopentadienyl), with a $\kappa(N,O)$ bidentate oximate ligand.[3]

* To whom correspondence should be addressed. E-mail: japm@uniovi.es. Fax: (34) 985103446.
[†] Universidad de Oviedo-CSIC.
[‡] Universidad de Valladolid.
[§] Instituto de Ciencia de Materiales de Madrid.
[£] European Synchrotron Radiation Facility.
[||] Universidad de Oviedo.

(1) (a) Singh, A.; Gupta, V. D.; Srivastava, G.; Mehrotra, R. C. *J. Organomet. Chem.* **1974**, *64*, 145. (b) Chakravorty, A. *Coord. Chem. Rev.* **1974**, *65*, 145. (c) Kukushkin, V. Y.; Tudela, D., Pombeiro, A. J. L. *Coord. Chem. Rev.* **1996**, *156*, 333. (d) Kukushkin, V. Y.; Pombeiro, A. J. L. *Coord. Chem. Rev.* **1999**, *181*, 147. (e) Mehrotra, R. C. In *Comprehensive Coordination Chemistry*; Wilkinson, G., Gillard, R. D., McCleverty, J. A., Eds.; Pergamon: Oxford, 2000; Vol. 2, pp 269−275. (f) Kukushkin, V. Y.; Pombeiro, A. J. L.; Mehrotra, R. C. In *Comprehensive Coordination Chemistry II*; McCleverty, J. A., Meyer, T. J., Eds.; Elsevier: Oxford, 2004; Vol 1, pp 631−637.

(2) (a) Khare, G. P.; Doedens, R. J. *Inorg. Chem.* **1976**, *15*, 86. (b) Aime, S.; Gervasio, G.; Milone, L.; Rossetti, R.; Stanghellini, P. L. *Chem. Commun.* **1976**, *11*, 370. (c) Aime, S.; Gervasio, G.; Milone, L.; Rossetti, R.; Stanghellini, P. L. *J. Chem. Soc., Dalton Trans.* **1978**, 534. (d) Carofligio, T.; Stella, S.; Floriani, C.; Chiesi-Villa, A.; Guastini, C. *J. Chem. Soc., Dalton Trans.* **1989**, 1957. (e) Deeming, A. J.; Owen, D. W.; Powell, N. I. *J. Organomet. Chem.* **1990**, *398*, 229. (f) Chao, M.; Kumaresan, S.; Wen, Y.; Lin, S.; Hwu, J. R.; Lu, K. *Organometallics* **2000**, *19*, 714. (g) Wong, J. S.; Wong, W. *New J. Chem.* **2002**, *26*, 94. (h) Cabeza, J. A., del Río, I.; Riera, V.; Suárez, M.; Alvarez-Rúa, C.; García-Granda, S.; Chuang, S. H.; Hwu, J. R. *Eur. J. Inorg. Chem.* **2003**, *23*, 4159.

(3) (a) Khare, G. P.; Doedens, R. J. *Inorg. Chem.* **1977**, *16*, 907. (b) King, R. B.; Chen, K. N. *Inorg. Chem.* **1977**, *16*, 1164. (c) For examples of mononuclear carbonyl oxime/oximato complexes with other metal fragments, see: Meyer, U.; Werner, H. *Chem. Ber.* **1990**, *123*, 697.

10.1021/ic062168c CCC: $37.00
Published on Web 02/14/2007

Scheme 1. Synthesis of the Oximato and Oxime Complexes, $[Re(ONCMe_2)(CO)_3(N-N)]$ (**1**−**2**) and $[Re\{N(OH)CMe_2\}(CO)_3(phen)]BAr'_4$ (**3**), Respectively; Transformation of the Latter into the Former by Deprotonation.

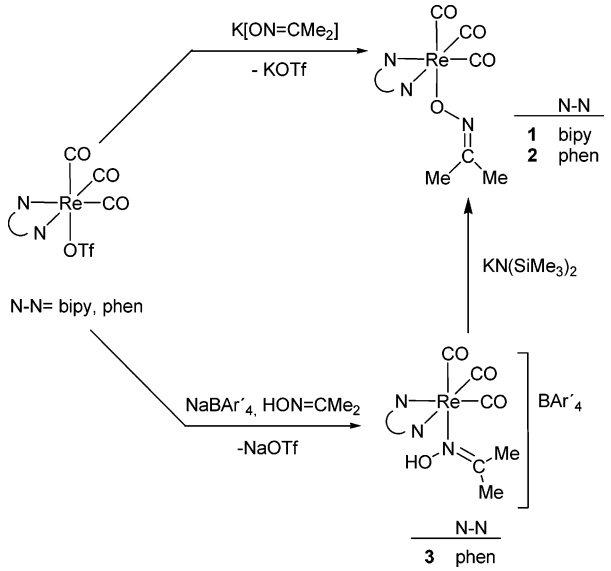

We have recently found that complexes $[ReX(CO)_3(N-N)]$ (N−N = 2,2′-bipyridine, bipy, or 1,10-phenanthroline, phen), where X is an anionic ligand with one or two lone electron pairs, such as alkoxo,[4] hydroxo,[5] amido,[6] alkylideneamido,[7] or phosphido,[8] display a rich X-based reactivity toward organic electrophiles. We set out to study if related complexes featuring terminal oximato ligands could be prepared and, if so, how they would react toward organic electrophiles. Our findings are reported in what follows.

Results and Discussion

Complexes $[Re(ONCMe_2)(CO)_3(bipy)]$ (**1**) and $[Re(ONCMe_2)(CO)_3(phen)]$ (**2**) were obtained as the single products of the reactions of in situ-generated $KONCMe_2$ with $[Re(OTf)(CO)_3(bipy)]$[4b] or $[Re(OTf)(CO)_3(phen)]$,[4b] respectively, in THF (see Scheme 1 and the Experimental Section). Precedents of this kind of synthetic procedure date back as early as 1970.[9]

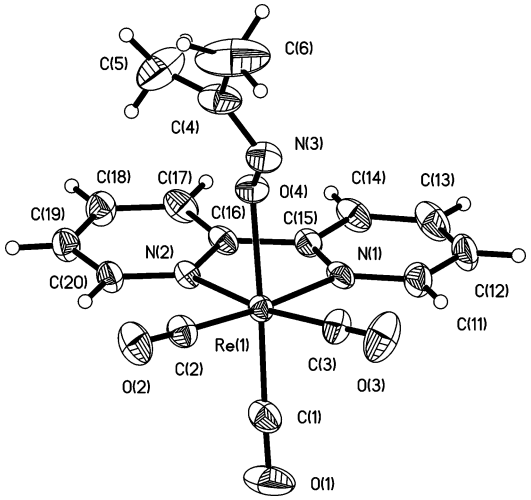

Figure 1. Thermal ellipsoid (30%) plot of $[Re(ONCMe_2)(CO)_3(bipy)]$ (**1**). Selected bond distances [Å] and angles [deg]: Re(1)−O(4) 2.079(4), N(3)−C(4) 1.282(9), N(3)−O(4) 1.368(6), N(3)−O(4)−Re(1) 118.2(3), C(4)−N(3)−O(4) 112.6(6).

In addition to spectroscopic characterization (see Experimental Section), single crystals grown by slow diffusion of diethyl ether into a THF solution of complex **1** were found to be suitable for X-ray diffraction, and the results of the structural determination are summarized in Figure 1. The molecule of **1** features an oximato ligand bound through its oxygen atom to a $\{Re(CO)_3(bipy)\}$ fragment and a Re−O distance, 2.079(4) Å, similar to that found in the methoxo complex $[Re(OMe)(CO)_3(bipy)]$ (2.081(5) Å).[10]

The monodentate coordination of the oximato ligand in compounds **1** and **2** is enforced by the lack of additional open metal coordination sites in these 18-electron products, and the preference for coordination through oxygen, the atom bearing the negative charge, over N-coordination, has been encountered for previously reported terminal oximato complexes.[1]

Since there is no significant difference in the reactivity of the $[ReX(CO)_3(N-N)]$ bipy and phen derivatives, in most of what follows only the chemistry of one of the oximato complexes will be discussed, and only one product of each type of reaction, the one for which X-ray quality crystals could be obtained, will be characterized.

To compare the complex of the anionic oximato ligand with that of the neutral oxime, we prepared $[Re(CO)_3(HONCMe_2)(phen)]BAr'_4$ (**3**) by the reaction of $[Re(OTf)(CO)_3(phen)]$, $HONCMe_2$, and $NaBAr'_4$ in CH_2Cl_2.[11] Compound **3** was characterized spectroscopically (see Experimental Section) and by X-ray diffraction (see Figure 2).

The main difference between the coordination geometry of this cationic complex and that of the neutral O-bonded oximato complex **1** discussed above is that the oxime ligand is coordinated to rhenium through its nitrogen atom. This coordination mode is the normally found for oxime complexes.[1] Comparison of the Re−N distance in **3** (2.183(6) Å) with those found in the compounds $[Re(CO)_3(bipy)(HN{=}CPh_2)]OTf$ (2.192(3) Å)[7a] and $[Re(CO)_3(bipy)(H_2N\textit{p}\text{-Tol})]$-

(4) (a) Hevia, E.; Pérez, J.; Riera, L.; Riera, V.; Miguel, D. *Organometallics* **2002**, *21*, 1750. (b) Hevia, E.; Pérez, J.; Riera, L.; Riera, V.; del Río, I.; García-Granda, S.; Miguel, D. *Chem. Eur. J.* **2002**, *8*, 4510.
(5) (a) Morales, D.; Navarro Clemente, M. E.; Pérez, J.; Riera, L.; Riera, V.; Miguel, D. *Organometallics* **2002**, *21*, 4934. (b) Gerbino, D. C.; Hevia, E.; Morales, D.; Navarro Clemente, M. E.; Pérez, J.; Riera, L.; Riera, V.; Miguel, D. *Chem. Commun.* **2003**, 328. (c) Cuesta, L.; Gerbino, D. C.; Hevia, E.; Morales, D.; Navarro Clemente, M. E.; Pérez, J.; Riera, L.; Riera, V.; Miguel, D.; del Río, I.; García-Granda, S. *Chem. Eur. J.* **2004**, *10*, 1765. (d) Cuesta, L.; Hevia, E.; Morales, D.; Pérez, J.; Riera, L.; Miguel, D. *Organometallics* **2006**, *25*, 1717.
(6) (a) Hevia, E.; Pérez, J.; Riera, V.; Miguel, D. *Organometallics* **2002**, *21*, 1966. (b) Hevia, E.; Pérez, J.; Riera, V.; Miguel, D. *Chem. Commun.* **2002**, 1814. (c) Hevia, E.; Pérez, J.; Riera, V.; Miguel, D. *Organometallics* **2003**, *22*, 257.
(7) (a) Hevia, E.; Pérez, J.; Riera, V.; Miguel, D. *Angew. Chem., Int. Ed.* **2002**, *20*, 3558. (b) Hevia, E.; Pérez, J.; Riera, V.; Miguel, D.; Campomanes, P.; Menéndez, M. I.; Sordo, T. L., García-Granda, S. *J. Am. Chem. Soc.* **2003**, *125*, 3706.
(8) (a) Cuesta, L.; Hevia, E.; Morales, D.; Pérez, J.; Riera, V.; Rodríguez, E.; Miguel, D. *Chem. Commun.* **2005**, 116. (b) Cuesta, L, Hevia, E.; Morales, D. Pérez, J.; Riera, V.; Seitz, M.; Miguel, D. *Organometallics* **2005**, *24*, 1772.
(9) Harrison, P. G.; Zuckerman, J. J. *Inorg. Chem.* **1970**, *9*, 175.
(10) Gibson, D. H.; Sleadd, B. A.; Yin, X. *Organometallics* **1998**, *17*, 2689.
(11) Hevia, E.; Pérez, J., Riera V.; Miguel, D. *Inorg. Chem.* **2002**, *41*, 4673.

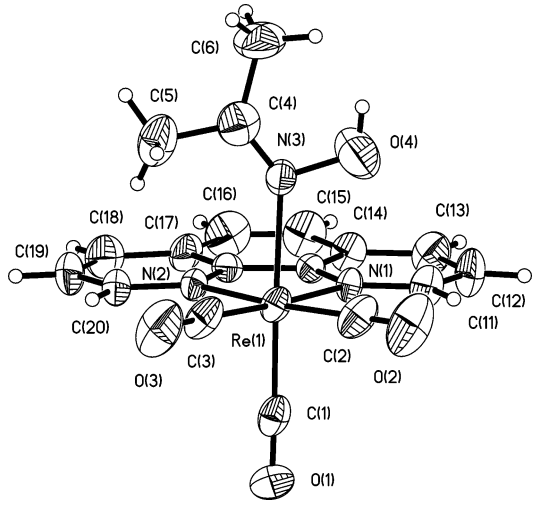

Figure 2. Thermal ellipsoid (30%) plot of the cation of [Re{N(OH)CMe_2}-$(CO)_3$(phen)]BAr'_4 (**3**). Selected bond distances [Å] and angles [deg]: Re(1)−N(1) 2.162(5), Re(1)−N(2) 2.170(5), Re(1)−N(3) 2.183(6), N(3)−O(4) 1.396(9), N(3)−C(4) 1.256(11), Re(1)−N(3)−O(4) 108.4(5), Re(1)−N(3)−C(4) 137.0(7).

OTf (2.250(3) Å)[6a] suggests that the oxime is a donor (σ-donor/π-aceptor) comparable to an imine and better than an amine. The Re−N(oxime) distance in **3** is short for a neutral ligand, since it is only slightly longer than the Re−N(phen) distances within the same complex (2.162(5) and 2.170(5) Å), suggesting that the oxime is a good ligand.

The synthesis of the oxime complex **3** contrasts with the oxidative addition of the N−O bond of $HONCMe_2$ to a highly electron-rich Re(I) center observed by Pombeiro and co-workers.[12]

Treatment of compound **3** with the strong base KN-$(SiMe_3)_2$ led to the instantaneous formation of the neutral oximato complex **2**, a transformation that illustrates the preference of oximato and oxime ligands for O- and N-coordination, respectively, as mentioned above.

Next, the reactivity of the oximato complexes toward the electrophiles *p*-tolylisocyanate, *p*-tolylisothiocyanate, maleic anhydride, tetracyanoethylene (TCNE), and dimethylacetylenedicarboxylate (DMAD) was studied.

Complex **2** reacted with the equimolar amount of *p*-tolylisocyanate [(*p*-Tol)NCO] in 1.5 h at room temperature, affording as the single product the new orange-colored complex [Re{N(*p*-Tol)C(O)$ONCMe_2$}$(CO)_3$(phen)] (**4**), resulting from the formal insertion of the isocyanate into the Re−O bond (Scheme 3).

The reaction was accompanied by a shift to higher wavenumber values of the IR ν_{CO} bands (at 2016, 1915, and 1889 cm^{-1} in THF solution in the product), consistent with the reaction of the metal carbonyl complex with an electrophile. The NMR data of compound **4** include two singlets at 2.11 and 1.61 ppm in ^{1}H NMR, assigned to the two inequivalent methyl groups from the oximato ligand, and two low-intensity singlets at 160.7 and 156.5 ppm in ^{13}C NMR, assigned to the C═O and C═N carbons, respectively, of the carbamato ligand formed. The structure of **4**, determined by X-ray diffraction, is displayed in Figure 3.

The pseudooctahedral molecule of **4** consists of a [N(*p*-Tol)C(O)$ONCMe_2$] ligand bonded through the nitrogen from (*p*-Tol)NCO to a {Re$(CO)_3$(phen)} fragment. The geometry about this nitrogen (labeled N(3) in Figure 3) is planar, indicating electronic delocalization (of the lone pair formally on nitrogen). The comparison between the distances N(3)−C(4) = 1.333(7) Å and N(3)−C(31) = 1.432(7) Å indicates that the delocalization involves the carbonyl group rather than the aryl group. A consequence of this delocalization is that **4** does not retain the nucleophilic character present in the oximato precursor, as it is demonstrated by the fact that **4** does not react with excess (*p*-Tol)NCO.

The preference for N-coordination over O-coordination observed in complex **4** can be rationalized on the basis of a softer character for the nitrogen atom, which would be a better match for the soft, low-oxidation, metal carbonyl fragment, in line with previous findings.[4b]

Compound **1** reacted also with the equimolar amount of *p*-tolylisothiocyanate ([(*p*-Tol)NCS], as shown in Scheme 3). The reaction took 8 h at room temperature (insofar as (*p*-Tol)NCS is less electrophilic than (*p*-Tol)NCO)[4b] and afforded as single product the new yellow complex [Re{SCN-(*p*-Tol)$ONCMe_2$}$(CO)_3$(bipy)] (**5**). As for compound **4** (see above), the spectroscopic data of **5** indicate the presence of the oximato and (*p*-Tol)NCS fragments, as well as the decrease in electron density of the metal center upon reaction with the isothiocyanate. The structure of **5** was determined by X-ray diffraction, and the results are shown in Figure 4.

The distances N(4)−C(4) = 1.24(2) Å and S(1)−C(4) = 1.73(1) Å are consistent with the double- and single-bond depictions, respectively, included in Scheme 2. The fact that the ligand resulting from the insertion of isothiocyanate into the Re−oximate bond is bonded to Re through S fits the simple soft/hard arguments mentioned above.

Complex **2** reacted with maleic anhydride over several hours to afford a mixture of two *fac*-tricarbonyl compounds, **6a** and **6b**, as judged by the IR monitoring of the reaction. Compound **6a** could be isolated by fractional crystallization and was characterized by IR, NMR, and X-ray diffraction (see Figure 5) as the complex [Re{OC(O)CH═CHC(O)-$ONCMe_2$}$(CO)_3$(phen)]. The X-ray determination of the structure of **6a** (Figure 5) confirms the formulation given above, resulting from ring-opening and insertion of maleic anhydride into the Re−O bond. The Re−O distance in **6a**, 2.140(3) Å, is longer than that in the starting oximato complex **2** (2.079(4) Å), likely a result of the lower donor capability of the carboxylato ligand bonded to the rhenium fragment in **6a** compared with the oximato ligand in complex **2,** also reflected in the substantial increase in IR ν_{CO} values.

The spectroscopic data of the byproduct **6b** featured IR ν_{CO} bands higher than those of **2**, and an AB system for the two nonequivalent olefinic hydrogens. We therefore suspected that **6b** could be the compound [Re{OC(O)CH═CHC(O)OH}$(CO)_3$(phen)], with a hydrogenmaleate ligand resulting from the acid−base reaction between the oximato complex **2** and maleic acid, present as a contaminant in the

(12) Ferreira, C. M. P.; Guedes da Silva, M. F. C.; Kukushkin, V. Y.; Fraústo da Silva, J. J. R.; Pombeiro, A. J. L. *Dalton Trans.* **1998**, 325.

Scheme 2. Reaction of the Oximato Complexes $[Re(ONCMe_2)(CO)_3(N-N)]$ (**1**−**2**) toward Different Organic Unsaturated Electrophiles

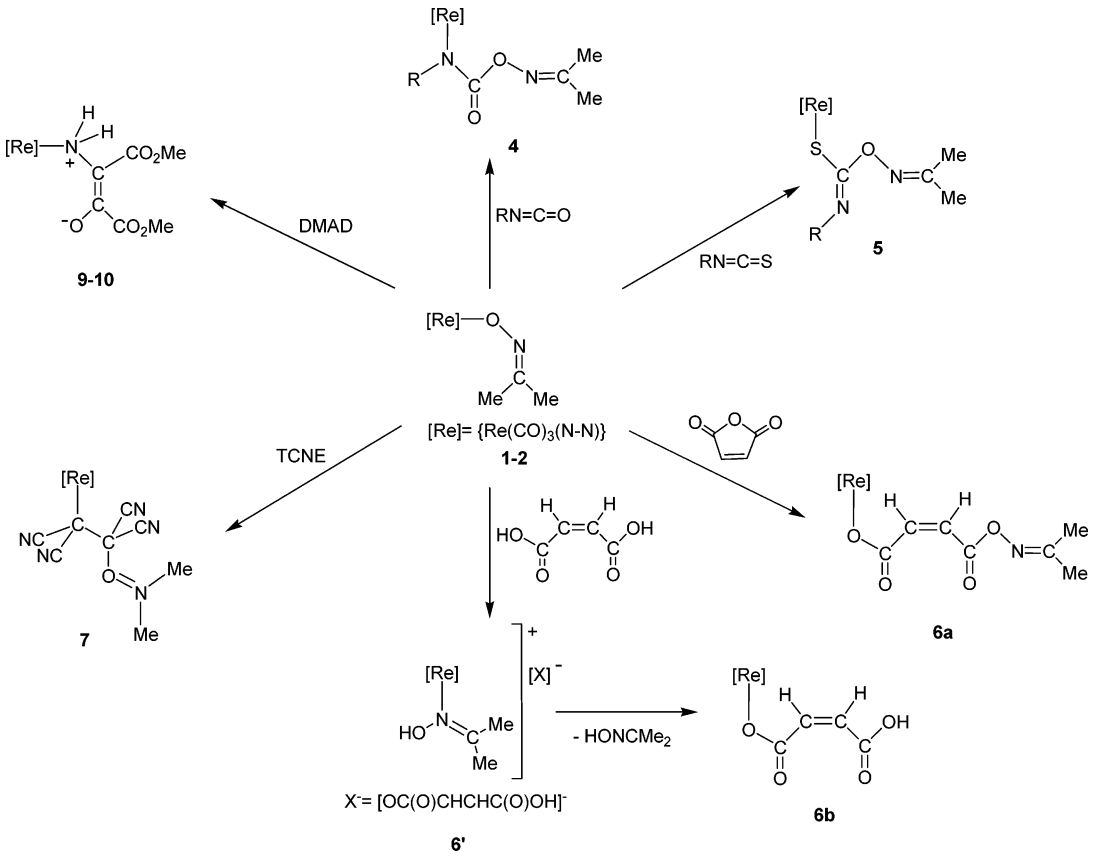

maleic anhydride due to its partial hydrolysis. To check this hypothesis, compound **2** was allowed to react with the equimolar amount of maleic acid. The reaction first afforded quantitatively the salt $[Re(CO)_3(phen)(HONCMe_2)][OC(O)CH{=}CHC(O)OH]$ (**6′**), the result of the protonation of the oximato ligand by maleic acid. Upon standing in solution several hours, **6′** was transformed into **6b**, the result of the displacement of the neutral oxime by the anionic hydrogenmaleate ligand (Scheme 2).

The addition of the equimolar amount of TCNE to a THF solution of complex **2** led to an instantaneous reaction, accompanied by a change in the color from red to yellow. The IR ν_{CO} bands shifted to higher frequencies by ca. 30 cm^{-1}. The IR spectrum of the resulting solution features also two low-intensity bands at 2216 and 2199 cm^{-1} assigned to the C−N stretches of the cyano groups (at 2253 cm^{-1} in free TCNE). A single product, complex **7**, could be characterized by IR and ^1H NMR (see Experimental Section). In addition, slow diffusion of hexane into a solution of **7** in CH_2Cl_2 at −20 °C afforded yellow crystals, one of which

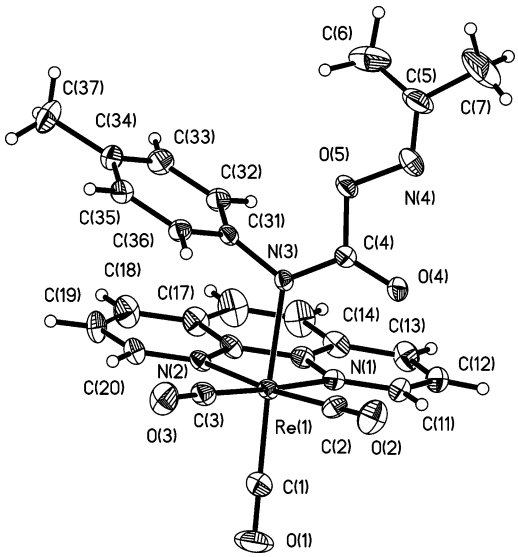

Figure 3. Thermal ellipsoid (30%) plot of $[Re\{N(p\text{-Tol})C(O)ONCMe_2\}(CO)_3(phen)]$ (**4**). Selected bond distances [Å] and angles [deg]: Re(1)−N(3) 2.192(5), N(3)−C(4) 1.333(7), N(3)−C(31) 1.432(7), Re(1)−C(31)−N(3) 120.5(3), Re(1)−C(4)−N(3) 119.5(4), C(4)−N(3)−C(31) 120.0(5).

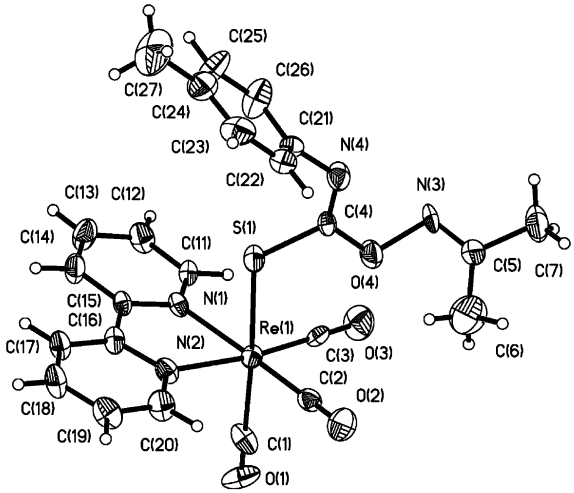

Figure 4. Thermal ellipsoid (30%) plot of $[Re\{SCN(p\text{-Tol})ONCMe_2\}(CO)_3(bipy)]$ (**5**). Selected bond distances [Å] and angles [deg]: Re(1)−S(1) 2.490(5), S(1)−C(4) 1.736(14), C(4)−N(4) 1.24(2), Re(1)−S(1)−C(4) 115.5(5).

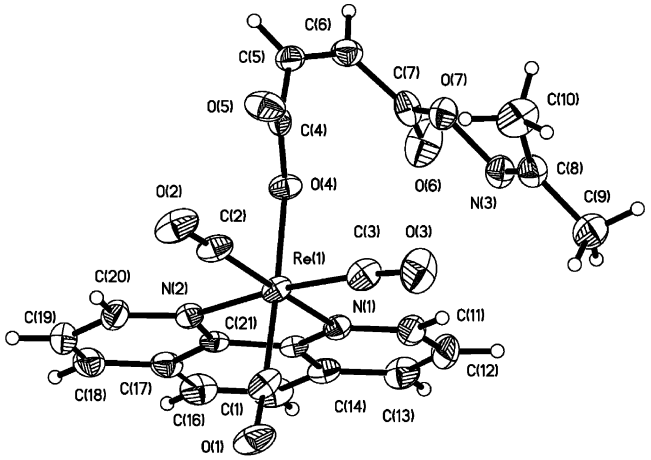

Figure 5. Thermal ellipsoid (30%) plot of [Re{OC(O)CH═CHC(O)-ONCMe$_2$}(CO)$_3$(phen)] (**6a**).

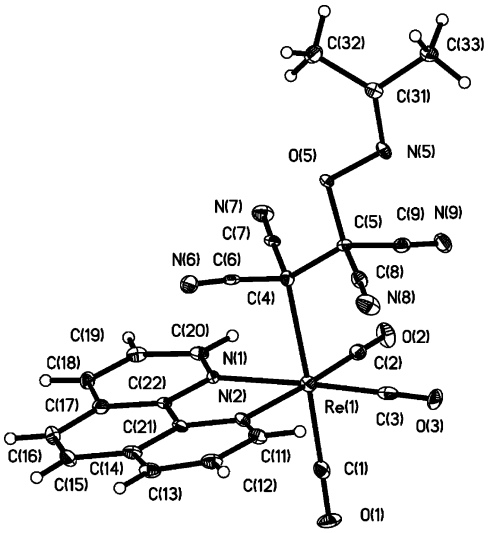

Figure 6. Thermal ellipsoid (30%) plot of [Re{C(CN)$_2$C(CN)$_2$ONCMe$_2$}-(CO)$_3$(phen)] (**7**). Selected bond distances [Å]: Re(1)−C(4) 2.359(5), C(4)−C(5) 1.547(7), C(5)−O(5) 1.419(6).

was employed for the structural determination by means of X-ray diffraction. The results, shown in Figure 6, indicate that **7** is the product of formal insertion of TCNE into the Re−O bond of the starting oximato complex. Accordingly, the distance C(4)−C(5) = 1.547(7) Å, is consistent with a single bond. The distance Re−C(4) = 2.359(5) Å is slightly longer than the Re−C distances found for other rhenium alkyl complexes, the same trend found when alkyl complexes of other metal fragments are compared with the related polycyanoalkyl complexes.[4b] Similar parameters were found in the compound [Re{C(CN)$_2$C(CN)$_2$(OMe)}(CO)$_3$(Me$_2$-bipy)], the product of the reaction of TCNE with the alkoxo complex [Re(OMe)(CO)$_3$(Me$_2$bipy)] (Me$_2$bipy = 4,4′-dimethyl-2,2′-bipyridine).[4b]

The oximato complex **2** reacted instantaneously with the equimolar amount of DMAD. The reaction yielded initially a single product, compound **8** (brown), which was isolated as a spectroscopically (IR and ^{1}H NMR) pure solid. When left in solution, compound **8** was found to quantitatively transform into a second species, **9** (yellow), in 8 h at room temperature.

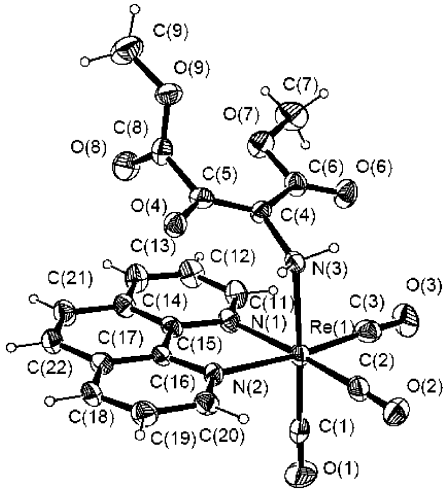

Figure 7. Thermal ellipsoid (30%) plot of [Re{NH$_2$C(CO$_2$Me)C(CO$_2$-Me)(O)}(CO)$_3$(phen)] (**9**). Selected bond distances [Å]: Re(1)−N(3) 2.237-(9), N(3)−C(4) 1.463(12), C(5)−O(4) 1.275(12), C(4)−C(6) 1.457(15), C(6)−O(6) 1.160(11), C(6)−O(7) 1.386(14), C(8)−O(8) 1.211(13), C(8)−O(9) 1.311(14).

When the reaction was carried out in CD_2Cl_2 in an NMR tube, ^{1}H NMR monitoring showed that the transformation of **8** into **9** was accompanied by the production of an equimolar amount of acetone, identified by the singlet at 2.12 ppm. Compound **9** was characterized by IR and ^{1}H NMR (its low solubility precluded the acquisition of a ^{13}C spectrum) and also by single-crystal X-ray diffraction. In agreement with the loss of acetone mentioned above, the ^{1}H NMR spectrum of **9** features only two methyl singlets, attributed to the two methoxycarbonyl groups from DMAD. The results of the structural determination are shown in Figure 7.

The molecule of **9** consists of a {Re(CO)$_3$(phen)} fragment bonded to the nitrogen atom of a [H$_2$NC(CO$_2$Me)═C(CO$_2$-Me)O] ligand. Given the structure of **9**, the observed formation of acetone upon transformation of **8** into **9** and the outcome of the reactions discussed above, we propose that the intermediate **8** is the product of the formal DMAD insertion into the Re−O bond depicted in Scheme 3. Accordingly, the ^{1}H NMR spectrum of **8** includes four methyl singlets; two of them, at higher frequencies, are assigned to the two methoxycarbonyl groups from the DMAD reagent, and the other two are assigned to the two nonequivalent oxime methyl groups. An alkenyl rhenium complex resulting from the reaction of DMAD with the rhenium methoxo complex [Re(OMe)(CO)$_3$(bipy)] was previously reported by us.[4a]

It was noted that the transformation of **8** into **9** required the presence of water (the addition of a large excess of water to a solution of **8** caused its instantaneous transformation into **9**). Since the source of the water involved in the formation of **9** must be the adventitious traces of water present in the reaction mixture, the reaction was repeated several times with solvents as anhydrous as we could get and with different batches of DMAD and oximato complex. The same result (slow formation of **9**) was consistently obtained. Furthermore, the formation of the analogous bipyridine complex [Re(NH$_2$C(CO$_2$Me)═C(CO$_2$Me)O)(CO)$_3$-

Scheme 3. Proposed Mechanism for the Transformation of Compound **8** into **9**.

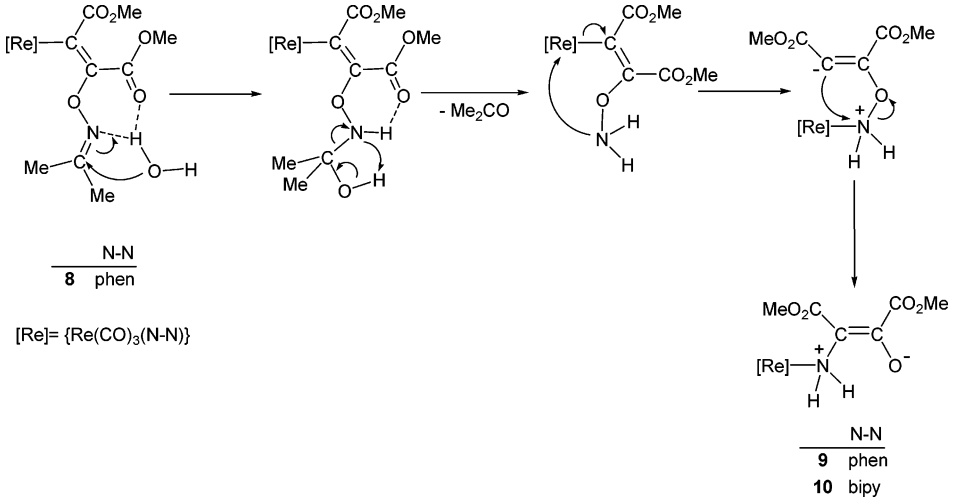

(bipy)] (**10**), the structure of which was confirmed by X-ray diffraction, was found when the oximato complex **1** was allowed to react with DMAD (see Experimental Section and Supporting Information).

A proposed rationale for the transformation of **8** (or its bipy analog) to **9**−**10**, admittedly a purely speculative one, is displayed in Scheme 3. The presence of the two strongly electron-withdrawing methoxycarbonyl groups in **8**, as well as the possible formation of a hydrogen bond to one of the hydrogen atoms of a molecule of water by the carbonyl oxygen of one of the −C(O)OMe groups, are factors that can explain the fact that **8** undergoes hydrolysis in conditions (only traces of water) in which other products of the reactions of the oximates **1** and **2**, also featuring the $-O-N{=}CMe_2$ moiety (described above), do not.

The final product, **9**, is depicted as a charge-separated tautomer, a situation rarely encountered for organometallic complexes. Experimental evidence in support of this formulation comes both from spectroscopic and X-ray diffraction data. Thus, the solution IR ν_{CO} bands in THF of **9** (2026 and 1919 cm^{-1}) and **10** (2026 and 1918 cm^{-1}) are closer to those of a cationic amino complex (2034 and 1925 cm^{-1} for $[Re(CO)_3(bipy)(H_2N\textit{p}\text{-Tol})]OTf$) than to those of a neutral amido complex (2003, 1899, and 1884 cm^{-1} for $[Re(HN\textit{p}\text{-Tol})(CO)_3(bipy)]$).[6a] In the solid state, the Re−N(3) distances (2.237(9) Å for **9** and 2.248(5) Å for **10**) are closer to the Re−N(amino) distance in $[Re(CO)_3(bipy)(H_2N\textit{p}\text{-Tol})]OTf$ (2.250(3) Å) than to the Re−N(amido) distance in $[Re(N\textit{p}\text{-Tol})(CO)_3(bipy)]$ (2.112(4) Å).[6a] This set of data suggest that the monodentate N-donor is an amino rather than an amido ligand. With regard to the oxygen atom to which we are assigning a negative charge, O(4), in complex **10** (in **9** the corresponding distances are known less accurately) the distance C(5)−O(4) (1.244(9) Å) is closer to the double bond C−O distances C(6)−O(6) (1.238(8) Å) and C(8)−O(8) (1.193(8) Å) than to the single bond C−O distances C(6)−O(7) (1.340(9) Å) and C(8)−O(9) (1.335(9) Å). This, and even the difference between the two double bond C−O distances mentioned above, are consistent with the delocalization depicted in Chart 1.

Chart 1. Electronic Delocalization in Compounds **9** and **10**.

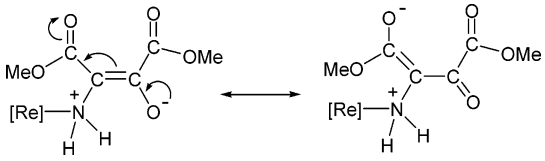

The preceding discussion is only based on comparisons between bond distances. To obtain a more clear picture of the bond orders, a topological analysis of the electron density as obtained from the Fourier map was carried out.[13] The results of this study afforded a picture consistent with that proposed in the preceding discussion. Thus, in **9**, the charge density is 2.017 e/Å^3 for the bond C(5)−O(4), intermediate between the values found for the double bonds C(6)−O(6) (2.234 e/Å^3) and C(8)−O(8) (2.291 e/Å^3) and those found for the single bonds (1.646 e/Å^3 for C(6)−O(7) and 1.893 e/Å^3 for C(8)−O(9)).

Likewise, in **10**, the charge density is 1.900 e/Å^3 for the bond C(5)−O(4), intermediate between the values found for the double bonds C(6)−O(6) (2.160 e/Å^3) and C(8)−O(8) (2.047 e/Å^3) and those found for the single bonds (1.707 e/Å^3 for C(6)−O(7) and 1.801 e/Å^3 for C(8)−O(9)).

When the intermolecular interactions are taken into account, the analysis of the X-ray diffraction data showed that both compounds **9** and **10** exist as dimers resulting from strong intermolecular hydrogen bonds in which the amino N−H bonds act as donors and the oxygen atom labeled O(4) is the acceptor (N(3)···O(4) = 2.81 Å and N(3)···H···O(4) = 146° for compound **9**), as shown in Figure 8.

An indication that such dimers maintain their integrity in solution comes from the low solubility of complexes **9** and **10** in moderately polar organic solvents such as CH_2Cl_2 or THF. Further evidence is provided by the presence of two separate low-intensity, broad signals in the ^{1}H NMR spectra of **9** and **10** for the two hydrogens of the NH_2 group of each complex. The inequivalence of these two hydrogen atoms (which would be equivalent in the monomeric C_s-symmetric

(13) Menéndez-Velázquez, A.; García-Granda, S. *J. Appl. Cryst.* **2003**, *36*, 193.

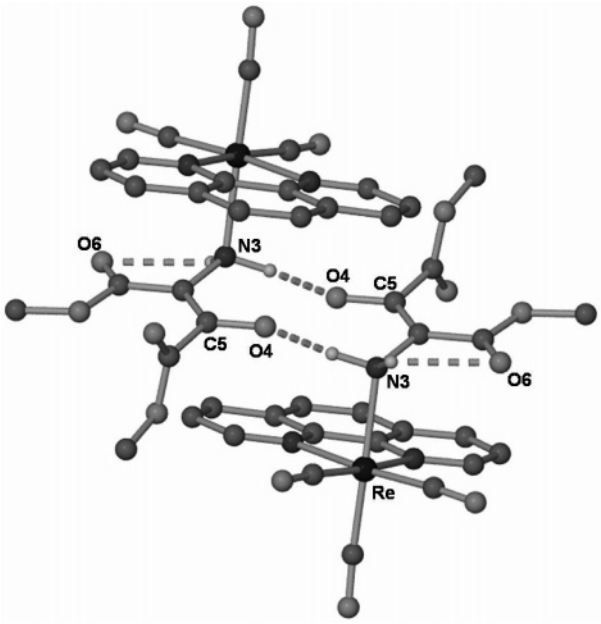

Figure 8. Hydrogen-bond interactions in the crystalline structure of **9** leading to dimers. Selected intermolecular distance and angle: N(3)···O(4) 2.81 Å, N(3)···H···O(4) 146°.

molecules) is attributed to their different involvement in the hydrogen-bonding scheme, depicted in Figure 8. Thus, one of the hydrogens on N(3) is involved in the mentioned intermolecular hydrogen bond, whereas the other forms an intramolecular hydrogen bond with O(6). In addition, the presence of the strong hydrogen bonds leading to the formation of the dimers should be a major factor in the stabilization of the charge-separated tautomer.

In summary, mononuclear complexes $[Re(ONCMe_2)(CO)_3(N{-}N)]$ (N−N = bipy or phen) containing O-coordinated oximato ligands, readily prepared by reaction of $[KON{=}CMe_2]$ with the respective triflato complexes, reacted with (*p*-Tol)-NCO, (*p*-Tol)NCS, maleic anhydride, TCNE, and DMAD, affording a single product in each case. The products have structures corresponding to the formal insertion of the electrophile into the Re−O bond. While the products of the first four reactions are stable, the product of the reaction with DMAD undergoes facile hydrolysis in the presence of the traces of water present in the solvents. This reaction is a complex process that involves addition of water, elimination of acetone, cleavage of the N−O bond, and formation of Re−N bond.

Experimental Section

All manipulations were carried out under a nitrogen atmosphere using conventional Schlenk techniques. Solvents were purified according to standard procedures.[14] $[Re(OTf)(CO)_3(N{-}N)]$ (N−N = bipy, phen)[4b] and $NaBAr'_4$[15] were prepared according to literature procedures. Other reagents were purchased and used as received. Deuterated solvents were stored under nitrogen in Young tubes. ^1H NMR and ^{13}C NMR spectra were recorded on a Bruker Advance 300, DPX-300, or Advance 400 spectrometer. NMR spectra are referred to the internal residual solvent peak for ^1H and $^{13}C\{^1H\}$ NMR. IR solution spectra were obtained in a Perkin-Elmer FT 1720-X or RX I FT-IR spectrometer using 0.2 mm. CaF_2 cells. Elemental analyses were performed on a Perkin-Elmer 2400B microanalyzer.

Synthesis of $[Re(ONCMe_2)(CO)_3(bipy)]$ (1). $KN(SiMe_3)_2$ (0.37 mL of a 0.5 M solution in toluene, 0.18 mmol) was added to a solution of acetone oxime (0.013 g, 0.17 mmol) in THF (10 mL) at −78 °C. The resulting colorless solution was transferred via canula to a solution of $[Re(OTf)(CO)_3(bipy)]$ (0.100 g, 0.17 mmol) in THF (10 mL). The color of the solution changed immediately from yellow to bright red. After 5 min the solvent was evaporated under reduced pressure, the residue was extracted with CH_2Cl_2 (10 mL), and filtered. The solvent was removed in vacuo to a volume of 5 mL and addition of hexane (20 mL) caused the precipitation of a red microcrystalline solid, which was washed with diethyl ether (2 × 5 mL) and redissolved in THF (5 mL). Slow diffusion of diethyl ether (10 mL) into this solution at room temperature afforded red crystals of **1**, one of which was employed for an X-ray structure determination. Yield: 0.062 g (69%). IR (THF, cm^{-1}): 2006 vs, 1903 s, 1876 s (ν_{CO}). ^1H NMR (CD_2Cl_2): δ 9.03, 8.21, 8.03, 7.51 (m, 2H each, bipy), 1.50 (s, 3H, C*H*$_3$), 1.12 (s, 3H, C*H*$_3$). Anal. Calcd for $C_{16}H_{14}N_3O_4Re$:C, 38.55; H, 2.83; N, 8.43. Found: C, 38.16; H, 3.13; N, 8.55.

Synthesis of $[Re(ONCMe_2)(CO)_3(phen)]$ (2). Compound **2** was prepared as described above for **1**, from $[Re(OTf)(CO)_3(phen)]$ (0.100 g, 0.17 mmol), $KN(SiMe_3)_2$ (0.37 mL of a 0.5 M solution in toluene, 0.18 mmol), and acetone oxime (0.013 g, 0.17 mmol). Slow diffusion of diethyl ether into a concentrated solution of **2** in THF at room temperature afforded red crystals. Yield: 0.066 g (71%). IR (THF, cm^{-1}): 2007 vs, 1903 s, 1877 s (ν_{CO}). ^1H NMR (CD_2Cl_2): δ 9.41 (dd, J = 5.1, 1.5 Hz, 2H, phen), 8.61 (dd, J = 8.2, 1.5 Hz, 2H, phen), 8.05 (s, 2H, phen), 7.89 (dd, J = 8.2, 5.1 Hz, 2H, phen), 1.42 (s, 3H, C*H*$_3$), 0.81 (s, 3H, C*H*$_3$). $^{13}C\{^1H\}$ NMR (CD_2Cl_2): δ 199.9 (2 × CO), 195.0 (CO), 150.1 (*C*═N), 152.7, 147.4, 137.9, 130.4, 127.3, 125.3 (phen), 20.9, 12.9 (2 × *C*H$_3$). Anal. Calcd for $C_{18}H_{14}N_3O_4Re$: C, 41.38; H, 2.70; N, 8.04. Found: C, 40.67; H, 3.01; N, 7.96.

Synthesis of $[Re\{N(OH)CMe_2\}(CO)_3(phen)]BAr'_4$ (3). To a solution of $[Re(OTf)(CO)_3(phen)]$ (0.050 g, 0.083 mmol) in CH_2Cl_2 (10 mL), $NaBAr'_4$ (0.074 g, 0.083 mmol), and acetone oxime (0.007 g, 0.092 mmol) were added. The mixture was stirred at room temperature for 5 min, filtered via canula, and the solvent was evaporated under reduced pressure to a volume of 5 mL. Slow diffusion of hexane (10 mL) into this solution at room temperature afforded yellow crystals of **3**, one of which was employed for an X-ray structure determination. Yield: 0.104 g (91%). IR (CH_2Cl_2, cm^{-1}): 2034 vs, 1932 s, 1923 s (ν_{CO}). ^1H NMR (CD_2Cl_2): δ 9.46 (dd, J = 5.2, 1.2 Hz, 2H, phen), 8.70 (dd, J = 8.3, 1.2 Hz, 2H, phen), 8.10 (s, 2H, phen), 8.00 (dd, J = 8.3, 5.2 Hz, 2H, phen), 7.74 (s, 8H, H$_o$ BAr′$_4$), 7.55 (s, 4H, H$_p$ BAr′$_4$), 5.56 (s, 1H, O*H*), 2.24 (s, 3H, C*H*$_3$), 1.86 (s, 3H, C*H*$_3$). $^{13}C\{^1H\}$ NMR (CD_2Cl_2): δ 194.3 (2 × CO), 189.6 (CO), 176.4 (*C*═N), 161.7 (c($^1J_{CB}$ = 50.1 Hz), *C*^{i} BAr′$_4$), 154.2, 147.1, 140.2, 131.2, 128.3, 126.6 (phen), 134.8 (*C*^{o} BAr′$_4$), 128.9 (c($^2J_{CF}$ = 31.5 Hz), *C*^{m} BAr′$_4$), 124.5 (c($^1J_{CF}$ = 272.7 Hz), *C*F$_3$ BAr′$_4$), 117.5 (*C*^{p} BAr′$_4$), 25.4, 19.2 (2 × *C*H$_3$). Anal. Calcd for $C_{50}H_{27}BF_{24}N_3O_4Re$: C, 43.31; H, 1.96; N, 3.03. Found: C, 43.58; H, 1.65; N, 3.15.

Synthesis of $[Re\{N(p\text{-}Tol)C(O)ONCMe_2\}(CO)_3(phen)]$ (4). (*p*-Tol)NCO (0.012 mL, 0.096 mmol) was added to a solution of $[Re(ONCMe_2)(CO)_3(phen)]$ (**2**) (0.050 g, 0.096 mmol) in THF (15 mL), and the mixture was stirred for 2 h. The color of the solution

(14) Perrin, D. D.; Armarego, W. L. F. *Purification of Laboratory Chemicals*, 3rd ed.; Pergamon Press: Oxford, 1988.
(15) (a) Brookhart, M.; Grant, B.; Volpe, A. F. *Organometallics* **1992**, *11*, 3920.

changed from red to orange. The solvent was evaporated under reduced pressure to a volume of 5 mL, and addition of hexane (15 mL) caused the precipitation of an orange microcrystalline solid, which was washed with hexane (2 × 5 mL) and diethyl ether (2 × 5 mL). Compound **4** was redissolved in 10 mL of CH_2Cl_2, and slow diffusion of diethyl ether (20 mL) at room temperature afforded orange crystals, one of which was employed for an X-ray analysis. Yield: 0.050 g (87%). IR (THF, cm^{-1}): 2016 vs, 1915 s, 1889 s (ν_{CO}). ^1H NMR (CD_2Cl_2): δ 9.11 (m, 2H, phen), 8.50 (dd, J = 8.2, 1.4 Hz, 2H, phen), 8.01 (s, 2H, phen), 7.66 (dd, J = 8.2, 5.3 Hz, 2H, phen), 6.49, 5.81, 5.79 (q, AA′BB′system, 4H, *p*-Tol), 2.11 (s, br, 6H, CH_3 *p*-Tol and CH_3 N═C(CH_3)$_2$), 1.61 (s, 3H, CH_3). $^{13}C\{^1H\}$ NMR (CD_2Cl_2): δ 200.7 (2 × CO), 195.6 (CO), 160.7 (*C*═O), 156.5 (*C*═N), 149.2, 140.0, 134.0, 132.7, 130.2, 129.6, 128.6, 127. 5 (*p*-Tol and phen), 27.3 (*C*H$_3$, *p*-Tol), 22.7, 17.5 (2 × *C*H$_3$). Anal. Calcd for $C_{26}H_{21}N_4O_5Re\cdot 0.25CH_2Cl_2$: C, 46.58; H, 3.20; N, 8.28. Found: C, 46.19; H, 3.11; N, 8.32.

Synthesis of [Re{SCN(*p*-Tol)(ONCMe$_2$)}(CO)$_3$(bipy)] (5). (*p*-Tol)NCS (0.012 mL, 0.096 mmol) was added to a solution of [Re(ONCMe$_2$)(CO)$_3$(bipy)] (**1**) (0.050 g, 0.096 mmol) in THF (15 mL), and the mixture was stirred for 8 h. The color of the solution changed from red to yellow. The solvent was evaporated under reduced pressure to a volume of 5 mL and addition of hexane (20 mL) caused the precipitation of a yellow microcrystalline solid, which was washed with hexane (2 × 10 mL) and diethyl ether (2 × 5 mL). Slow diffusion of hexane (10 mL) into a concentrated solution of **5** in CH_2Cl_2 at room temperature afforded yellow crystals, one of which was employed for an X-ray analysis. Yield: 0.054 g (87%). IR (CH_2Cl_2, cm^{-1}): 2017 vs, 1917 s, 1898 s (ν_{CO}). ^1H NMR (CD_2Cl_2): δ 8.98 (m, 2H, bipy), 8.44 (m, 2H, bipy), 8.02 (m, 2H, bipy), 7.50 (m, 2H, bipy), 6.82, 6.79, 6.40, 6.37 (q, AA′BB′system, 4H, *p*-Tol), 2.15 (s, 3H, CH_3), 2.12 (s, 3H, CH_3), 2.03 (s, 3H, CH_3). $^{13}C\{^1H\}$ NMR (CD_2Cl_2): δ 163.3 (*C*═N), 157.6, 155.7, 150.8, 141.13, 133.0, 131.0, 129.4, 125.6, 123.9 (bipy and *p*-Tol), 24.2 (*C*H$_3$, *p*-Tol), 22.8, 19.7 (2 × *C*H$_3$). Low solubility of **5** precluded the observation of the weak Re−*C*O signals. Anal. Calcd for $C_{24}H_{21}N_4O_4ReS$:C, 44.44; H, 3.27; N, 8.64. Found: C, 44.76; H, 3.61; N, 8.55.

Synthesis of [Re{OC(O)CH═CHC(O)ONCMe$_2$}(CO)$_3$(phen)] (6a). To a solution of [Re(ONCMe$_2$)(CO)$_3$(phen)] (**2**) (0.050 g, 0.096 mmol) in THF (15 mL), maleic anhydride (0.010 g, 0.100 mmol) was added and the mixture was stirred for 12 h. The color of the solution changed from red to yellow. The solvent was evaporated under reduced pressure to a volume of 5 mL, and addition of hexane (20 mL) caused the precipitation of a yellow solid, which was washed with hexane (2 × 10 mL). Slow diffusion of diethyl ether (20 mL) into a concentrated solution of **6a** in CH_2Cl_2 at room temperature afforded yellow crystals, one of which was employed for an X-ray determination. Yield: 0.041 g (68%). IR (THF, cm^{-1}): 2019 vs, 1917 s, 1891 s (ν_{CO}). ^1H NMR (CD_2Cl_2): δ 9.48 (dd, J = 5.1, 1.4 Hz, 2H, phen), 8.63 (dd, J = 8.3, 1.4 Hz, 2H, phen), 8.07 (s, 2H, phen), 7.91 (dd, J = 8.3, 5.1 Hz, 2H, phen), 5.85, 5.57 (AB system, 2H, *H*C═C*H*), 2.06 (s, 3H, CH_3), 1.92 (s, 3H, CH_3). Anal. Calcd for $C_{22}H_{16}N_3O_7Re$: C, 42.58; H, 2.60; N, 6.67. Found: C, 41.26; H, 2.69; N, 6.75.

Synthesis of [Re{N(OH)CMe$_2$}(CO)$_3$(phen)][OC(O)CH═CHC(O)OH] (6′). To a solution of [Re(ONCMe$_2$)(CO)$_3$(phen)] (**2**) (0.020 g, 0.037 mmol) in THF (10 mL) maleic acid (0.004 g, mmol) was added. The color of the solution changed immediately from red to pale orange, and the mixture was stirred at room temperature for 15 min. The solvent was evaporated under reduced pressure to a volume of 5 mL, and addition of hexane (15 mL) caused the precipitation of a yellow solid, which was washed with hexane (2 × 10 mL) and diethyl ether (2 × 10 mL). Yield: 0.022 g (93%). IR (THF, cm^{-1}): 2029 vs, 1926 s, 1916 s (ν_{CO}). ^1H NMR (CD_2Cl_2): δ 9.42 (m, 2H, phen), 8.66 (m, 2H, phen), 8.06 (s, 2H, phen), 7.92 (dd, J = 8.2, 5.1 Hz, 2H, phen), 5.84 (s, 2H, *H*C═C*H*), 2.32 (s, 3H, CH_3), 1.89 (s, 3H, CH_3).

Synthesis of [Re{OC(O)CH═CHC(O)OH}(CO)$_3$(phen)] (6b). Compound **6′** (0.022 g, 0.034 mmol) was dissolved in THF (10 mL), and the light orange solution was stirred at room temperature for 5 h. The solvent was evaporated under reduced pressure to a volume of 5 mL and addition of hexane (15 mL) caused the precipitation of a yellow solid, which was washed with hexane (2 × 10 mL) and diethyl ether (2 × 10 mL). Yield: 0.018 g (91%). IR (THF, cm^{-1}): 2025 vs, 1924 s, 1905 s (ν_{CO}). ^1H NMR (CD_2Cl_2): δ 9.48 (dd, J = 5.1, 1.4 Hz, 2H, phen), 8.66 (dd, J = 8.2, 1.4 Hz, 2H, phen), 8.09 (s, 2H, phen), 7.95 (dd, J = 6.2, 5.1 Hz, 2H, phen), 5.80, 5.71 (AB system, 2H, *H*C═C*H*). Anal. Calcd for $C_{19}H_{11}N_2O_7Re$: C, 40.35; H, 1.96; N, 4.95. Found: C, 39.98; H, 2.21; N, 5.14.

Synthesis of [Re{C(CN)$_2$C(CN)$_2$ONCMe$_2$}(CO)$_3$(phen)] (7). Tetracyanoethylene (0.012 g, 0.096 mmol) was added to a solution of [Re(ONCMe$_2$)(CO)$_3$(phen)] (**2**) (0.050 g, 0.096 mmol) in THF (15 mL) at −78 °C. Immediately, the color of the solution changed from red to yellow. The solvent was evaporated under reduced pressure to a volume of 5 mL and addition of hexane (15 mL) caused the precipitation of a yellow solid, which was washed with hexane (2 × 10 mL). Slow diffusion of hexane (10 mL) into a concentrated solution of **7** in CH_2Cl_2 at −20 °C afforded yellow crystals, one of which was employed for an X-ray analysis. Yield: 0.062 g (88%). IR (CH_2Cl_2, cm^{-1}): 2216w, 2199w (ν_{CN}); 2033 vs, 1931 s (ν_{CO}). ^1H NMR (CD_2Cl_2): δ 9.45 (dd, J = 5.1, 1.4 Hz, 2H, phen), 8.69 (dd, J = 8.2, 1.4 Hz, 2H, phen), 8.14 (s, 2H, phen), 8.00 (dd, J = 8.2, 5.1 Hz, 2H, phen), 2.01 (s, 3H, CH_3), 1.97 (s, 3H, CH_3). Anal. Calcd for $C_{24}H_{14}N_7O_4Re\cdot CH_2Cl_2$: C, 40.82; H, 2.19; N, 13.33. Found: C, 41.16; H, 1.90; N, 13.82.

Synthesis of [Re{C(CO$_2$Me)C═C(CO$_2$Me)(ONCMe$_2$}(CO)$_3$(phen)] (8). DMAD (0.012 mL, 0.097 mmol) was added to a solution of **2** (0.050 g, 0.096 mmol) in THF (15 mL). The color of the solution changed immediately from red to light brown. The solvent was evaporated under reduced pressure to a volume of 5 mL, and addition of hexane (15 mL) caused the precipitation of a brown solid, which was washed with hexane (2 × 10 mL) and diethyl ether (2 × 10 mL). Yield: 0.047 g (74%). IR (THF, cm^{-1}): 2020vs, 1917s, 1895s (ν_{CO}). ^1H NMR ($(CD_3)_2CO$): δ 9.45 (m, 2H, phen), 9.00 (m, 2H, phen), 8.36 (s, 2H, phen), 8.19 (dd, J = 8.1, 5.1 Hz, 2H, phen), 3.77 (s, 3H, CO$_2$CH_3), 3.34 (s, 3H, CO$_2$CH_3), 1.06 (s, 3H, CH_3), 0.66 (s, 3H, CH_3).

Synthesis of [Re{NH$_2$C(CO$_2$Me)C(CO$_2$Me)(O)}(CO)$_3$(phen)] (9). Attempts to crystallize compound **8** at room temperature by slow diffusion of hexane (15 mL) in a concentrated solution of **8** in CH_2Cl_2 afforded yellow crystals. One of these crystals was employed for an X-ray determination which showed a hydrolysis reaction had occurred affording compound **9**. Yield: 0.011 g (18%). IR (THF, cm^{-1}): 2020vs, 1917s, 1895s (ν_{CO}). ^1H NMR ($(CD_3)_2CO$): δ 9.44 (dd, J = 5.2, 1.3 Hz, 2H, phen), 8.90 (dd, J = 8.2, 1.3 Hz, 2H, phen), 8.25 (s, 2H, phen), 8.07 (dd, J = 8.2, 5.2 Hz, 2H, phen), 4.68 (s, br, 1H, N*H* of NH$_2$), 3.28 (s, 3H, CO$_2$CH_3), 3.10 (s, br, N*H* of NH$_2$), 2.82 (s, 3H, CO$_2$CH_3). Anal. Calcd for $C_{21}H_{16}N_3O_8Re$: C, 40.38; H, 2.58; N, 6.73. Found: C, 40.63; H, 2.49; N, 6.49.

Synthesis of [Re{NH$_2$C(CO$_2$Me)C(CO$_2$Me)(O)}(CO)$_3$(bipy)] (10). To a solution of **1** (0.050 g, 0.096 mmol) in THF (15 mL), DMAD (12 μL, 0.097 mmol) was added and the mixture was stirred at room temperature for 8 h. The color of the solution changed

Table 1. Selected Crystal, Measurement and Refinement Data for Compounds **1**, **3**, **4**, **5**, **6a**, **7**, **9**, and **10**.

	1	**3**	**4**	**5**
formula	$C_{16}H_{14}N_3O_4Re$	$C_{50}H_{27}BF_{24}N_3O_4Re$	$C_{26}H_{21}N_4O_5Re°0.25CH_2Cl_2$	$C_{24}H_{21}N_4O_4ReS$
fw	498.50	1386.76	676.90	647.71
cryst syst	monoclinic	monoclinic	triclinic	monoclinic
space group	$P2_1$	$P2_1/n$	$P\bar{1}$	$P2_1/n$
a, Å	6.665(2)	20.177(5)	9.984(3)	6.559(5)
b, Å	14.740(5)	13.770(3)	11.569(4)	18.448(14)
c, Å	8.779(3)	20.177(5)	13.526(5)	22.006(17)
α, deg	90	90	103.207(6)	90
β, deg	91.498(6)	111.696(3)	11.490(5)	90.758(14)
γ, deg	90	90	95.130(6)	90
V, Å^3	862.2(5)	5209(2)	1389.3(8)	2663(4)
Z	2	4	2	4
F(000)	476	2704	661	1264
D_{calcd}, g cm^{-3}	2.412	1.768	1.618	1.616
radiation (*λ*, Å)	Mo Kα, 0.71073	Mo Kα, 0.71073	Mo Kα, 0.71073	Mo Kα, 0.71073
μ, mm^{-1}	7.071	2.467	4.462	4.677
cryst size, mm^3	0.22 × 0.17 × 0.13	0.45 × 0.11 × 0.07	0.44 × 0.35 × 0.32	0.31 × 0.10 × 0.04
T, K	296(2)	296(2)	293(2)	296(2)
θ limits, deg	2.32−23.27	1.22−23.31	1.84−23.26	1.44−23.26
min/max *h*, *k*, *l*	−7/7, −16/16, −9/5	−22/22, −15/15, −21/22	−11/11, −12/12, −11/14	−7/6, −16/20, −22/24
collected reflns	3813	23 260	6026	11 795
unique reflns	2430	7506	3877	3800
absorption	SADABS	SADABS	SADABS	SADABS
params/restraints	219/1	741/0	335/0	311/0
GOF on F^2	1.016	1.012	1.023	1.163
R1 (on *F*, $I > 2\sigma(I)$)	0.0171	0.0431	0.0288	0.0724
wR2 (on F^2, all data)	0.0420	0.1238	0.0861	0.1791
max/min Δ*ρ*, e Å^{-3}	0.532 and −0.337	0.907 and −0.977	1.863 and −1.863	1.846 and −3.889
	6a	**7**	**9**	**10**
formula	$C_{22}H_{16}N_3O_7Re$	$C_{24}H_{12}N_7O_4Re°CH_2Cl_2$	$C_{21}H_{20}N_3O_{10}Re$	$C_{19}H_{16}N_3O_8Re$
fw	620.58	735.55	660.61	600.55
cryst syst	monoclinic	triclinic	Monoclinic	Triclinic
space group	$C2/c$	$P\bar{1}$	$P\ 2_1/c$	$P\ -1$
a, Å	24.471(14)	7.7302(15)	9.2206(3)	8.374(3)
b, Å	10.101(5)	11.292(2)	20.4832(8)	10.639(4)
c, Å	20.223(10)	16.019(3)	13.3466(6)	13.446(5)
α, deg	90	88.46(3)	90	103.459(7)
β, deg	129.629(7)	77.65(3)	94.792(2)	106.804(7)
γ, deg	90	76.79(3)	90	105.346(7)
V, Å^3	4480(4)	1329.5(5)	2511.9(2)	1041.9(7)
Z	8	2	4	2
F(000)	2400	712	1288	580
D_{calcd}, g cm^{-3}	1.840	1.837	1.747	1.914
radiation (*λ*, Å)	Mo Kα, 0.71073	Mo Kα, 0.71073	Cu Kα, 1.54184	Mo Kα, 0.71073
μ, mm^{-1}	5.474	4.817	9.978	5.883
cryst size, mm^3	0.27 × 0.15 × 0.06	0.20 × 0.10 × 0.07	0.27 × 0.15 × 0.17	0.15 × 0.07 × 0.04
T, K	296(2)	293(2)	293(2)	296(2)
θ limits, deg	1.86−23.32	1.30−25.68	4.0 to 68.2	1.68 to 23.41
min/max *h*, *k*, *l*	−25/31, −11/9, −22/22	−9/9, −13/13, −18/19	−10/11, 0/23, 0/16	−9/9, −11/11, −8/14
collected reflns	9651	7131	21166	4738
unique reflns	3215	4860	4387	2998
absorption	SADABS	multi scan	SORTAV	SADABS
params/restraints	300/0	355/0	331/12	282/0
GOF on F^2	1.020	1.089	1.110	1.021
R1 (on *F*, $I > 2\sigma(I)$)	0.0240	0.0408	0.0544	0.0361
wR2 (on F^2, all data)	0.0542	0.1057	0.1638	0.0546
max/min Δ*ρ*, e Å^{-3}	0.694 and −0.564	1.890 and −1.728	1.130 and −1.271	0.808 and −0.869

from red to yellow. The solvent was evaporated under reduced pressure to a volume of 5 mL, and addition of hexane (20 mL) caused the precipitation of a yellow solid, which was washed with diethyl ether (2 × 5 mL). Slow diffusion of diethyl ether (20 mL) into a concentrated solution of **10** in CH_2Cl_2 at room temperature afforded crystals, one of which was employed for an X-ray determination. Yield: 0.037 g, 64%. IR (CH_2Cl_2, cm^{-1}): 2026vs, 1919s (ν_{CO}). ^{1}H NMR ($(CD_3)_2CO$): δ 9.04 (m, 2H, bipy), 8.56 (m, 2H, bipy), 8.25 (m, 2H, bipy), 7.68 (m, 2H, bipy), 4.63 (s, br, 1H, N*H* of NH_2), 3.38 (s, 3H, CO_2CH_3), 3.20 (s, br, 1H, N*H* of NH_2), 2.98 (s, 3H, CO_2CH_3). Anal. Calcd for $C_{19}H_{16}N_3O_8Re$: C, 38.00; H, 2.69; N, 7.00. Found: C, 37.61; H, 2.77; N, 7.19.

Crystal Structure Determination for Compounds 1, 3, 4, 5, 6a, 7, 9, and 10. General Description. A suitable crystal was attached to a glass fiber and transferred to a Bruker AXS SMART 1000 (Nonius Kappa CCD for **9**) diffractometer with graphite-monochromatized Mo Kα (Cu Kα for **9**) X-ray radiation and a CCD area detector. One hemisphere of the reciprocal space was collected in each case. Raw frame data were integrated with the SAINT[16] (HKL Denzo and Scalepack[17] for **9**) program. The

(16) *SAINT+. SAX area detector integration program. Version 6.02*; Bruker AXS, Inc.: Madison, WI, 1999.
(17) Otwinowski, Z.; Minor, W. *Methods Enzymol.* **1997**, *276*, 307.

structures were solved by direct methods with SHELXTL.[18] An empirical absorption correction was applied with the program SADABS[19] (SORTAV[20] for **9**). All non-hydrogen atoms were refined anisotropically. Hydrogen atoms were set in calculated positions and refined as riding atoms. Drawings and other calculations were made with SHELXTL (ORTEP[21] and X-Seed[20] for **9** and **10**). Crystal and refinement details are collected in Table 1.

(18) Sheldrick, G. M. *SHELXTL, An integrated system for solving, refining, and displaying crystal structures from diffraction data. Version 5.1*; Bruker AXS, Inc.: Madison, WI, 1998.
(19) Sheldrick, G. M. *SADABS, Empirical Absorption Correction Program*; University of Göttingen: Göttingen, Germany, 1997.
(20) Blessing, R. H. *Acta Crystallogr.* **1995**, *A51*, 33.
(21) Farrugia, L. J. *J. Appl. Crystallogr.* **1997**, *30*, 565.
(22) Barbour, L. J. *J. Supramol. Chem.* **2001**, *1*, 189.

Acknowledgment. We thank Ministerio de Ciencia y Tecnología (grants CTQ2006-08924, MAT2006-1997, BQU2003-08649, and CTQ2006-07036/BQU) and Junta de Castilla y León (Grant No. VA012C05) for support of this work, and Ministerio de Educación y Ciencia for a FPU predoctoral fellowship (to L.C.) and for Ramón y Cajal contracts (to D. Morales and L.R.).

Supporting Information Available: X-ray crystallographic data for compounds **1**, **3**, **4**, **5**, **6a**, **7**, **9**, and **10** as CIF. This material is available free of charge via the Internet at http://pubs.acs.org.

IC062168C